

POWER SPECTRA FOR COLD DARK MATTER AND ITS VARIANTS

DANIEL J. EISENSTEIN AND WAYNE HU¹
Institute for Advanced Study, Princeton, NJ 08540
Received 1997 October 13; accepted 1998 August 27

ABSTRACT

The bulk of recent cosmological research has focused on the adiabatic cold dark matter model and its simple extensions. Here we present an accurate fitting formula that describes the matter transfer functions of all common variants, including mixed dark matter models. The result is a function of wavenumber, time, and six cosmological parameters: the massive neutrino density, number of neutrino species degenerate in mass, baryon density, Hubble constant, cosmological constant, and spatial curvature. We show how observational constraints—e.g., the shape of the power spectrum, the abundance of clusters and damped Ly α systems, and the properties of the Ly α forest—can be extended to a wide range of cosmologies, which includes variations in the neutrino and baryon fractions in both high-density and low-density universes.

Subject headings: cosmology: theory — dark matter — large-scale structure of universe

1. INTRODUCTION

Most popular cosmologies rely on density perturbations generated in the early universe and amplified by gravity to produce the structure observed in the universe such as galaxies, galaxy clustering, and the anisotropy of the microwave background. It is of particular interest that the spectrum and evolution of these fluctuations depend on the nature of the dark matter as well as upon the “classical” cosmological parameters. Hence, by the study of the observable signatures of the perturbations, one hopes to learn not only about quantities such as the density of the universe or the Hubble constant, but also what fraction of the matter in the universe is in baryons, cold dark matter (CDM), massive neutrinos, and so forth.

The calculation of how the various types of dark matter and the background cosmology affect the power spectrum can be treated for much of the history of the universe using linear perturbation theory. Numerically, this reduces to integrating the coupled Boltzmann equations for each mode as a function of time. For modes above the Jeans scales of the gravitating species, the growth of perturbations is independent of scale. In the absence of hot or warm dark matter, this scale drops precipitously after recombination, and therefore the late-time power spectrum may be separated into a function of scale and a scale-independent growth function that incorporates the effects of time, cosmological constant, and curvature. These growth functions are well cataloged (see, e.g., Peebles 1980), while the form of the spatial function can be found numerically (see, e.g., Bond & Efstathiou 1984) or quoted from fitting forms (see, e.g., Bond & Efstathiou 1984; Bardeen et al. 1986; Holtzman 1989; Eisenstein & Hu 1998, hereafter EH98).

With the introduction of massive neutrinos (Fang, Li, & Xiang 1984; Valdarnini & Bonometto 1985; Achilli, Occhionero, & Scaramella 1985) or other forms of hot dark matter, the spatial and temporal behavior of the perturbations cannot be separated. The Jeans scale, also called the free-streaming scale, of the neutrinos remains significant after recombination (Bond & Szalay 1983). In this case, the

CDM and baryon perturbations are not traced by neutrinos and grow more slowly because of the reduction of the gravitational source (Bond, Efstathiou, & Silk 1980). Since the free-streaming scale itself moves to ever smaller scales with increasing time, the transfer function acquires a non-trivial time dependence. Consequently, a cosmological constant or nonzero curvature enters the problem in a more complicated manner. Although accurate numerical treatments exist (Ma & Bertschinger 1995; Dodelson, Gates, & Stebbins 1996a), these complications have meant that fitting formula (Holtzman 1989; Klypin et al. 1993; Pogosyan & Starobinsky 1995; Ma 1996) for the power spectra of such cosmologies have been restricted to certain regions of parameter space; e.g., fixed baryon content and critical density overall.

In Hu & Eisenstein (1998, hereafter HE98), we showed that the late-time evolution of perturbations in a mixed dark matter (MDM) cosmology with CDM, baryons, and massive neutrinos could be accurately treated using a scale-dependent growth function. The transfer function then becomes the product of this growth function and a time-independent master function that represents the perturbations around recombination. Moreover, the small-scale limit of this master function can be calculated analytically as a function of cosmological parameters (HE98).

In this paper, we give an accurate fitting formula for the master function.² This in turn produces a fitting formula for the transfer functions of adiabatic cosmologies as functions of matter density, baryon and neutrino fractions, cosmological constant, Hubble constant, redshift, and the number of degenerate massive neutrino species. For the central region of parameter space, i.e., only moderate deviations from the pure CDM model, the formula is accurate to better than 5% in the transfer function (10% in power). The formula does not attempt to fit the acoustic oscillations created by large baryon fractions, but it does provide a

² The formulae in § 3 of this paper are available in electronic form at <http://www.sns.ias.edu/~whu/transfer/transfer.html>. We also include a driver that calculates *COBE*-normalized σ_8 and other constraints from § 5 as a function of cosmological input parameters.

¹ Alfred P. Sloan Fellow.

good match to the underlying smooth function. Hence the formula loses accuracy for baryon fractions exceeding 30%. Similarly, the formula has larger errors for cosmologies with massive neutrino fractions exceeding 30% or with matter densities outside the range $0.06 \lesssim \Omega_0 h^2 \lesssim 0.4$; however, if the baryon fraction is less than 10% in this range, the accuracy improves to better than 3%.

The outline of the paper is as follows. In § 2 we review the basic results of linear perturbation theory. We then present the fitting function in § 3 and a user's guide in § 4. As illustrative examples of the utility of the formula in exploring parameter space, we examine constraints on large-scale structure and high-redshift objects in § 5. We conclude in § 6.

2. DESCRIPTION OF PHYSICAL SITUATION

We consider linear adiabatic perturbations around a Friedmann-Robertson-Walker metric for cosmologies with several species of particles: photons, baryons (i.e., nuclei and electrons), massive and massless neutrinos, and CDM. The interaction between this diverse set of particles can lead to complex phenomenology in the growth of perturbations, even in linear theory (see, e.g., Peebles 1993).

Nevertheless, the underlying physical situation remains simple. Perturbations under the so-called Jeans scale are not subject to gravitational instability due to pressure support or, in the case of collisionless particles, sufficient rms velocity. Above this scale, perturbations grow at the same rate regardless of scale. In general, the Jeans scale of each gravitating species is imprinted into the power spectrum. It is conventional to define the transfer function as the ratio of time-integrated growth on a particular scale as compared with that on scales far larger than the Jeans scale.

For a relativistic species, the Jeans scale grows with the particle horizon. In a universe with CDM and radiation only, the Jeans scale of the total system grows to the size of the horizon at matter-radiation equality and then shrinks to zero as the universe becomes matter dominated. The result is that the transfer function turns over at the scale of the horizon at equality. Moreover, well after equality the Jeans scale has dropped sufficiently that all scales of interest are above it and hence grow at the same rate. The familiar result is that the spectrum of fluctuations can be written at low redshifts as a scale-independent growth factor times a function of scale that depends only on the size of the horizon at equality.

With the inclusion of the baryons, another scale is imprinted in the transfer function. The baryons are dynamically coupled to the photons until the end of the Compton drag epoch, close to recombination for the standard thermal history. Prior to this time, the baryonic Jeans scale tracks the horizon (or more properly the sound horizon, which accounts for the fact that baryons contribute mass but little pressure). After recombination, the Jeans scale of the baryons drops precipitously to scales smaller than those of interest for large-scale structure (for sub-Jeans perturbations, see Yamamoto, Sugiyama, & Sato 1998). The sound horizon at the end of the Compton drag epoch is thereby imprinted in the transfer function in the form of Jeans or acoustic oscillations (see EH98). Again, perturbations at low redshifts grow at the same rate on all relevant scales.

The same principles may be applied to massive neutrinos. At sufficiently high temperatures, even massive neutrinos

behave as radiation; therefore their Jeans scale grows with the horizon. As their temperature drops with the expansion, they become nonrelativistic and their Jeans scale shrinks. Physically, their momenta decay with the expansion and eventually become small enough to allow them to cluster with the nonrelativistic matter. For this reason the Jeans scale is often called the free-streaming scale. By the same arguments as before, the maximal free-streaming scale is imprinted in the transfer function. What makes the massive neutrino case more complicated than the CDM and radiation case is that for eV-mass neutrinos the free-streaming scale *today* lies in the regime of large-scale structure measurements. Thus the growth of fluctuations in the regime of interest is not independent of scale, even at low redshifts.

Let us examine the growth in more detail. A given scale begins outside the free-streaming length; here the neutrino density perturbation traces those of the other species. If the scale is below the maximal free-streaming scale, it will at some point cross the free-streaming scale. While in the free-streaming regime, perturbations in the neutrinos damp out collisionlessly while those in the CDM and baryons grow more slowly because of the loss of a gravitating source. As the neutrinos slow down and their Jeans scale shrinks, the scale in question eventually crosses back out of the free-streaming regime. At this time the neutrinos fall back into the potential wells of the other species, and the growth rate is boosted back to its original rate. Even at low redshifts, some scales are still in the free-streaming regime; hence, the temporal and spatial dependence of the transfer function cannot be separated as before.

If all of the massive neutrinos had the same momentum, then one could hope to describe the free-streaming situation more exactly, but of course the neutrinos have a thermal distribution, which was frozen in when the universe had a temperature of about 1 MeV. Hence the transition between free-streaming and infall occurs smoothly and requires a Boltzmann code to follow (Ma & Bertschinger 1995). HE98 showed that the result could be well fitted by a scale-dependent growth rate; we will use this here to separate the time dependence from the complications of the spatial dependences.

3. FITTING FORM

3.1. Scales and Notation

We begin by describing our notation. The density of CDM, baryons, and massive neutrinos, in units of the critical density, are denoted Ω_c , Ω_b , and Ω_ν , respectively. The total matter density is then $\Omega_0 = \Omega_c + \Omega_b + \Omega_\nu$. f_c, f_b , and f_ν are the ratio of the density of these species to the total Ω_0 . We use multiple subscripts to indicate summation so that, e.g., $f_{cb} = f_c + f_b = (\Omega_c + \Omega_b)/\Omega_0$. The contribution of a cosmological constant Λ is written as $\Omega_\Lambda \equiv \Lambda/3H_0^2$ and is not included in Ω_0 . The Hubble constant is parameterized as $H_0 = 100 h \text{ km s}^{-1} \text{ Mpc}^{-1}$. The CMB temperature is given by $T_{\text{CMB}} = 2.7\Theta_{2.7} \text{ K}$; the best determination to date is $2.728 \pm 0.004 \text{ K}$ (Fixsen et al. 1996; 95% confidence interval), at which it is fixed for most of our expressions.

We assume that there are three species of neutrinos with a temperature equal to $(4/11)^{1/3}$ of the photons while they are relativistic. One or more of the species may be sufficiently massive to influence cosmology, but we only study the case where the most massive species have essentially equal masses. Then N_ν is the number of these species, and the

mass of each is $m_\nu = 91.5\Omega_\nu h^2 N_\nu^{-1} \text{ eV } c^{-2}$ (Kolb & Turner 1990).

We generally work with the redshift z as our time coordinate. The redshift of matter-radiation equality is³

$$z_{\text{eq}} = 2.50 \times 10^4 \Omega_0 h^2 \Theta_{2.7}^{-4}. \quad (1)$$

The baryons are released from the Compton drag of the photons near recombination at a redshift (see Hu & Sugiyama 1996; EH98)

$$z_d = 1291 \frac{(\Omega_0 h^2)^{0.251}}{1 + 0.659(\Omega_0 h^2)^{0.828}} [1 + b_1(\Omega_b h^2)^{b_2}],$$

$$b_1 = 0.313(\Omega_0 h^2)^{-0.419} [1 + 0.607(\Omega_0 h^2)^{0.674}],$$

$$b_2 = 0.238(\Omega_0 h^2)^{0.223}. \quad (2)$$

However, it is more convenient to label this epoch by the relative expansion since matter-radiation equality, so we define

$$y_d = \frac{1 + z_{\text{eq}}}{1 + z_d}. \quad (3)$$

The comoving distance that a sound wave can propagate prior to z_d is called the sound horizon and is (EH98)

$$s = \frac{44.5 \ln(9.83/\Omega_0 h^2)}{\sqrt{1 + 10(\Omega_b h^2)^{3/4}}} \text{ Mpc} \quad (4)$$

(note that the units are Mpc, not h^{-1} Mpc).

As we are using linear perturbation theory, it is appropriate to work in Fourier space where the transfer function depends on the comoving wavenumber k . We often parameterize k relative to the scale that crosses the horizon at matter-radiation equality, so as to define

$$q = \frac{k}{\text{Mpc}^{-1}} \Theta_{2.7}^2 (\Omega_0 h^2)^{-1}$$

$$= \frac{k}{19.0} (\Omega_0 H_0^2)^{-1/2} (1 + z_{\text{eq}})^{-1/2}. \quad (5)$$

3.2. Free-Streaming and Infall

As shown in HE98, one can decompose the transfer function into a scale-dependent growth function that incorporates all postrecombination effects and a time-independent master function that reflects conditions at the drag epoch. Hence, we write the transfer function of the density-weighted CDM and baryon perturbations as

$$T_{cb}(q, z) = T_{\text{master}}(q) D_{cb}(q, z) / D_1(z), \quad (6)$$

and that of the density-weighted CDM, baryon, and neutrino perturbations as

$$T_{cb\nu}(q, z) = T_{\text{master}}(q) D_{cb\nu}(q, z) / D_1(z). \quad (7)$$

Here, D_1 is the growth factor for the universe in the absence of neutrino free-streaming (i.e., on very large scales), D_{cb} and $D_{cb\nu}$ are the scale-dependent MDM growth functions, and T_{master} is the time-independent master function. We describe these now in turn.

In the absence of free-streaming, the growth function takes on the usual form (Heath 1977; Peebles 1980)

$$D_1(z) = \frac{5\Omega_0}{2} (1 + z_{\text{eq}}) g(z) \int^z \frac{1 + z'}{g(z')^3} dz', \quad (8)$$

$$g^2(z) = \Omega_0(1 + z)^3 + (1 - \Omega_0 - \Omega_\Lambda)(1 + z)^2 + \Omega_\Lambda. \quad (9)$$

We have chosen the normalization to be $D_1 = (1 + z_{\text{eq}})/(1 + z)$ at early times. For an $\Omega_0 = 1$ universe, equation (8) yields $D_1 = (1 + z_{\text{eq}})/(1 + z)$ at all times; closed form expressions are also available for universes without Λ (Weinberg 1972; Edwards & Heath 1976; Groth & Peebles 1975) and flat low-density universes with Λ (Bildhauer, Buchert, & Kasai 1992). Alternatively one may use the fitting form (Lahav et al. 1991; Carroll, Press, & Turner 1992)

$$D_1(z) = \left(\frac{1 + z_{\text{eq}}}{1 + z} \right) \frac{5\Omega(z)}{2} \left\{ \Omega(z)^{4/7} - \Omega_\Lambda(z) \right. \\ \left. + \left[1 + \frac{\Omega(z)}{2} \right] \left[1 + \frac{\Omega_\Lambda(z)}{70} \right] \right\}^{-1},$$

$$\Omega(z) = \Omega_0(1 + z)^3 g^{-2}(z),$$

$$\Omega_\Lambda(z) = \Omega_\Lambda g^{-2}(z), \quad (10)$$

where $g(z)$ is defined in equation (9).

The presence of neutrinos suppresses the growth of fluctuations on scales sufficiently small that the neutrinos' velocity allows them to escape the perturbation. This alters the logarithmic growth rate (Bond et al. 1980) according to the factor ($i = cb, c$)

$$p_i \equiv \frac{1}{4} [5 - \sqrt{1 + 24f_i}] \geq 0. \quad (11)$$

Then the growth rates in the presence of free streaming are (HE98)

$$D_{cb}(z, q) = \left[\frac{1 + D_1(z)}{1 + y_{\text{fs}}(q; f_\nu)} \right]^{p_{cb}/0.7} D_1(z)^{1 - p_{cb}}, \quad (12)$$

and

$$D_{cb\nu}(z, q) = \left\{ f_{cb}^{0.7/p_{cb}} + \left[\frac{D_1(z)}{1 + y_{\text{fs}}(q; f_\nu)} \right] \right\}^{p_{cb}/0.7} D_1(z)^{1 - p_{cb}}, \quad (13)$$

for the CDM + baryon and CDM + baryon + neutrino cases, respectively. In both cases, the free-streaming epoch as a function of scale is

$$y_{\text{fs}}(q) = 17.2 f_\nu (1 + 0.488 f_\nu^{-7/6}) (N_\nu q / f_\nu)^2. \quad (14)$$

Note that increasing N_ν at fixed Ω_ν prolongs free streaming by making the neutrinos less massive and hence faster moving.

The functions D_{cb} and $D_{cb\nu}$ contain all the dependence of the transfer functions on time, curvature, and cosmological constant, and moreover relate the two transfer functions to a single master function. Of course, in a cosmology with no massive neutrinos, $D_{cb} = D_{cb\nu} = D_1$ and the master function is simply the usual postrecombination transfer function.

3.3. The Master Function

The master function reflects the spectrum of perturbations at the drag epoch. As such, it can only depend on

³ Although this is not well defined in cases with $\Omega_\nu \neq 0$, we justify our choice in HE98.

$\Omega_0 h^2, f_b, f_v,$ and N_v . In the case without massive neutrinos, this reduces to the CDM + baryon transfer function. EH98 described the phenomenology of this function. In particular, the presence of baryons suppresses power on scales smaller than the sound horizon at the drag epoch and introduces a series of oscillations in the transfer function that damp as one moves to smaller scales. For moderate baryon fractions ($f_b \lesssim \Omega_0 h^2 + 0.2$), the oscillations are fairly small but the suppression can be important (roughly $5f_b$ in power). Because of the increased complexity of adding massive neutrinos to the form, we opt not to fit the oscillations and instead tailor a formula that runs through the center of the oscillations and properly incorporates the small-scale suppression. Of course, this means that the formula will not be appropriate for cases where the oscillations are large, roughly $\Omega_b/(\Omega_c + \Omega_b) \gtrsim \Omega_0 h^2 + 0.2$.

On scales much larger than the sound horizon at the drag epoch and the horizon at the time when the neutrinos finally become nonrelativistic, the effects of pressure fluctuations and collisionless damping are not important. Therefore, the transfer function will match that of a pure CDM model. On small scales, we have solved the evolution equations analytically and therefore can calculate the amount of small-scale suppression due to the baryons and neutrinos (HE98). We use these two limits to anchor our fitting form.

The suppression of power in the master function on small scales is primarily due to baryons, although neutrinos do contribute a residual coefficient not included in the free-streaming growth function.⁴ The amount of small-scale suppression is given as (HE98)

$$\begin{aligned} \alpha_v(f_v, f_b, y_d) &= \frac{f_c}{f_{cb}} \frac{5 - 2(p_c + p_{cb})}{5 - 4p_{cb}} \\ &\times \frac{1 - 0.553f_{vb} + 0.126f_{vb}^3}{1 - 0.193\sqrt{f_v}N_v + 0.169f_v N_v^{0.2}} (1 + y_d)^{p_{cb} - p_c} \\ &\times \left\{ 1 + \frac{p_c - p_{cb}}{2} \left[1 + \frac{1}{(3 - 4p_c)(7 - 4p_{cb})} \right] (1 + y_d)^{-1} \right\}. \end{aligned} \quad (15)$$

We choose to include this suppression by a scale-dependent rescaling of the zero baryon shape parameter Γ (see EH98). The suppression occurs rapidly near the sound horizon (defined in eq. [4]):

$$\Gamma_{\text{eff}} = \Omega_0 h^2 \left[\sqrt{\alpha_v} + \frac{1 - \sqrt{\alpha_v}}{1 + (0.43ks)^4} \right], \quad (16)$$

$$q_{\text{eff}} = \frac{k\Theta_{2.7}^2}{\Gamma_{\text{eff}} \text{Mpc}^{-1}}. \quad (17)$$

Then we use this effective wavenumber in the zero baryon form,

$$T_{\text{sup}}(k) = \frac{L}{L + Cq_{\text{eff}}^2}, \quad (18)$$

$$L = \ln(e + 1.84\beta_c \sqrt{\alpha_v} q_{\text{eff}}), \quad (19)$$

$$C = 14.4 + \frac{325}{1 + 60.5q_{\text{eff}}^{1.11}}, \quad (20)$$

⁴ The total suppression of T_{cb} on small scales is $\alpha_v D_{-1}^{p_{cb}}$.

$$\beta_c = (1 - 0.949f_{vb})^{-1}, \quad (21)$$

to produce a form that breaks from the large-scale, pure CDM formula to the small-scale solution.

We find, however, that this formula is inaccurate around the scale of the horizon at the epoch when the neutrinos slowed to nonrelativistic speeds, the so-called maximal free-streaming scale (see § 2). This is because the form of y_{fs} (eq. [14]) assumes that the neutrino velocity scales simply as $v \propto (1 + z)$. In fact, it is the momentum that carries this scaling, while the velocity cannot exceed c . This error causes us to overestimate the maximal free-streaming scale (note that in eq. [14] the running of this scale with redshift is cutoff at the equality epoch). In turn, the growth functions D_{cb} and D_{cbv} provide too much free-streaming suppression on these scales, although since the scales are well above the free-streaming scale for $z \lesssim 30$, no spurious time dependence is introduced at late times.

For $f_v \leq 0.3$, this error can be fixed by the following multiplicative correction:

$$B(k) = 1 + \frac{1.2f_v^{0.64} N_v^{0.3 + 0.6f_v}}{q_v^{-1.6} + q_v^{0.8}}; \quad (22)$$

$$q_v = \frac{k}{3.42\sqrt{f_v/N_v} k_{\text{eq}}} = \frac{3.92q\sqrt{N_v}}{f_v}. \quad (23)$$

The master function is then

$$T_{\text{master}}(k) = T_{\text{sup}}(k)B(k). \quad (24)$$

3.4. Performance

In Figures 1 and 2, we compare the fitting formula to the numerical evaluation (using the CMB fast code of Seljak & Zaldarriaga 1996, version 2.3) of the transfer function. Figure 1 shows the most common MDM model— $\Omega_0 = 1$, $h = 0.5$, $\Omega_b = 0.05$, $\Omega_v = 0.2$, and $N_v = 1$ —at two different redshifts. Figure 2 shows other cases—high baryon fraction, low Ω_0 , $N_v = 2$, and high $\Omega_0 h^2$ —at redshift zero.

For $0.06 \lesssim \Omega_0 h^2 \lesssim 0.40$, $\Omega_b/\Omega_0 \leq 0.3$, $\Omega_v/\Omega_0 \leq 0.3$, $z = 0$, and $N_v = 1$, the accuracy of the fitting formula is quite high. For baryon fractions of 5%, the acoustic oscillations are small and the fit is better than 2% on all scales. At higher baryon fractions, the oscillations become more prominent, and therefore the maximum level of the residuals grows, although the residuals would at least partially cancel for many applications. Performance for $f_b \leq 0.3$ is nearly always better than 5% (and often $\lesssim 3\%$) when comparing with the nonoscillatory portion of the transfer function. The small-scale fit for $q > 0.25$ ($k \gtrsim 1 \text{ Mpc}^{-1}$) is always better than 2% accurate. Behavior for $N_v = 2$ is similar, although different numerical codes seem to be inconsistent for $q \gg 1$ at the several percent level. Performance at $z = 9$ is at most 1% worse than that at $z = 0$; at $z = 29$, performance can degrade by 4% at the lowest values of $\Omega_0 h^2$ (where z/z_{eq} is its largest). Hence 5% accuracy is achieved only for $z < 30$.

For $\Omega_0 h^2 \gtrsim 0.4$, the fitting formula tends to overestimate the transfer function on scales just below the sound horizon ($k \approx 0.3 \text{ Mpc}^{-1}$) and underestimate it just above the sound horizon ($k \approx 0.1 \text{ Mpc}^{-1}$); we display this problem in Figure 2d. These errors are only a few percent for $f_b < 0.1$, but grow to 10% by $f_b \approx 0.3$. The culprit is our reliance on using an effective Γ within a pure-CDM transfer function; for high $\Omega_0 h^2$ the sound horizon corresponds to $q \ll 1$, thereby altering the portion of the curve we use for our transition

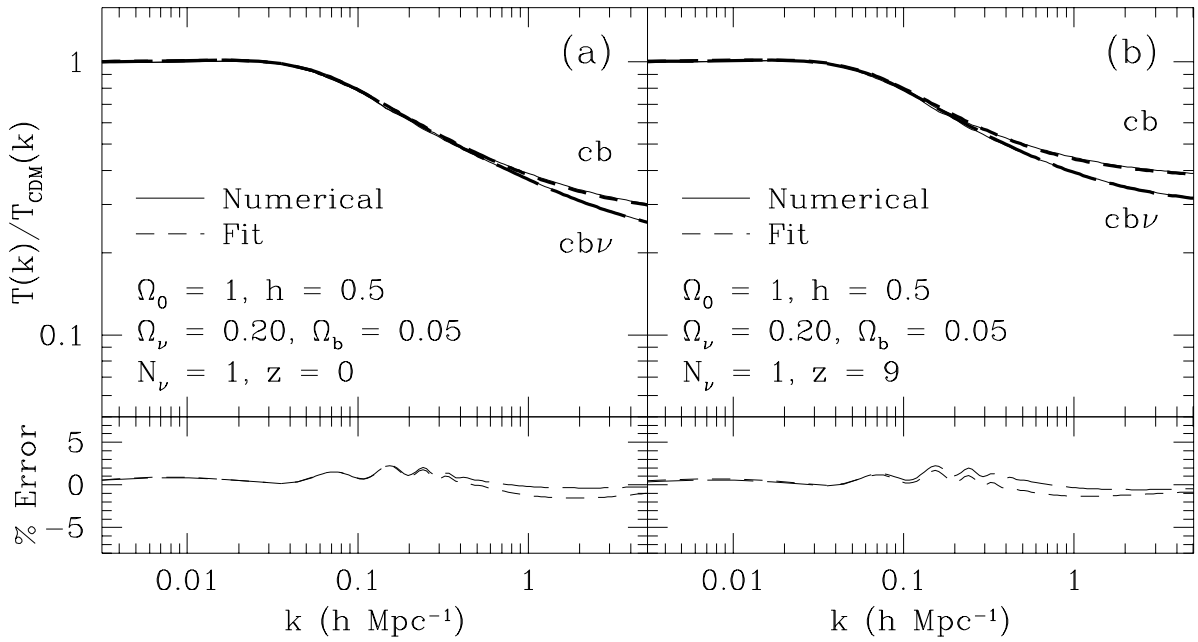


FIG. 1.—Comparison of the fitting formula to the numerical results of CMB fast (Seljak & Zaldarriaga 1996). Results at (a) $z = 0$, (b) $z = 9$. *Upper panels:* Transfer functions divided by a fiducial pure CDM transfer function, formed by using eq. (18) with $\alpha_v = \beta_c = 1$ and $q_{\text{eff}} = q$. Density-weighted CDM + baryon (short-dashed line) and CDM + baryon + neutrino (long-dashed line) transfer functions are shown. *Lower panels:* Fractional residuals. The cosmology is $\Omega_0 = 1$, $\Omega_v = 0.2$, $\Omega_b = 0.05$, and $h = 0.5$.

(eq. [16]). For $\Omega_0 h^2 \lesssim 0.06$, the opposite situation occurs; moreover, the power series in $1 + y_d$ in equation (15) becomes less accurate. For $\Omega_0 h^2 = 0.025$, the errors are 5% for both low and moderate baryon fractions.

For models with $\Omega_b/(\Omega_b + \Omega_c) \gtrsim \Omega_0 h^2 + 0.2$, the baryon oscillations exceed 10% in amplitude, which may be a problem for some applications. By $\Omega_0 h^2 + 0.4$, the oscillations are of order 40% (see Fig. 5 of EH98). We note that the location of the peaks in wavenumber seems essentially constant with varying Ω_b ; thus the formulae in EH98 could be used to give the location but not the amplitude.

For neutrino fractions exceeding 30%, our correction for the behavior near the maximal free-streaming scale (eq. [23]) is too small, which leads to significant errors (8% for $f_v \approx 0.5$, and increasing thereafter).

For $\Omega_0 < 1$, we have only tested the fit on intermediate scales for flat universes (i.e., $\Omega_\Lambda = 1 - \Omega_0$). We have tested the small-scale limit in both open and flat cases and found excellent accuracy.

Note that our formula works equally well for cases with $\Omega_v = 0$. Of course, in this case, should one wish to fit the baryon oscillations, one should use the fitting formula in EH98.

4. USER'S GUIDE

We present here a user's guide to the fitting formulae of the previous section. The fitting formula for the density-weighted matter transfer function, with and without neutrinos, is given by equations (1)–(24). For cases with $\Omega_v \neq 0$, these functions are time dependent and involve the growth factors in equations (12) and (13). We now detail how to use the transfer function to construct power spectra and measures of mass fluctuations.

4.1. Power Spectra

The power spectrum is constructed from the transfer functions in the usual way:

$$\frac{k^3}{2\pi^2} P(k, z) = \delta_H^2 \left(\frac{ck}{H_0} \right)^{3+n} \frac{T^2(k, z) D_1^2(z)}{D_1^2(0)}, \quad (25)$$

where δ_H is the amplitude of perturbations on the horizon scale today, and n is the initial power spectrum index, which is equal to 1 for a scale-invariant spectrum. Note that the usual growth function D_1 from equation (8) is used, not D_{cb} or $D_{cb\nu}$.

In cases with $\Omega_v \neq 0$, there are three transfer functions, and hence three power spectra, that may be constructed. Using T_{cb} from equation (6) in equation (25) yields P_{cb} , the power spectra for the CDM and baryons. Likewise using $T_{cb\nu}$ from equation (7) yields $P_{cb\nu}$, the density-weighted power spectrum of the CDM, baryons, and massive neutrinos. The power spectrum of the massive neutrinos themselves can be constructed from the functions above. One can subtract the transfer functions given above to find the transfer function for the neutrinos alone:

$$T_v = f_v^{-1} (T_{cb\nu} - f_{cb} T_{cb}). \quad (26)$$

On small scales this function goes to zero, but we have not carefully modeled this. Thus, T_v has density-weighted errors similar to those in T_{cb} ; that is, the residuals in the fit for $f_v T_v$ will be similar to those of T_{cb} . This transfer function may be employed in equation (25) to obtain P_v , the power spectrum of the massive neutrinos.

Power spectra for velocity fields can be similarly obtained by considering the continuity equation, which relates them to time derivatives of the density fluctuations. It is standard to express this in terms of the quantity $f \equiv -d \log(D)/d \log(1+z)$, where D is the growth function. In a model with massive neutrinos, this becomes a scale-dependent quantity. We can differentiate equation (12) directly to find

$$f_{cb}(k, z) = f_0(z) \left\{ 1 - \frac{P_{cb}}{1 + [D_1(z)/(1 + y_{fs})]^{0.7}} \right\}, \quad (27)$$

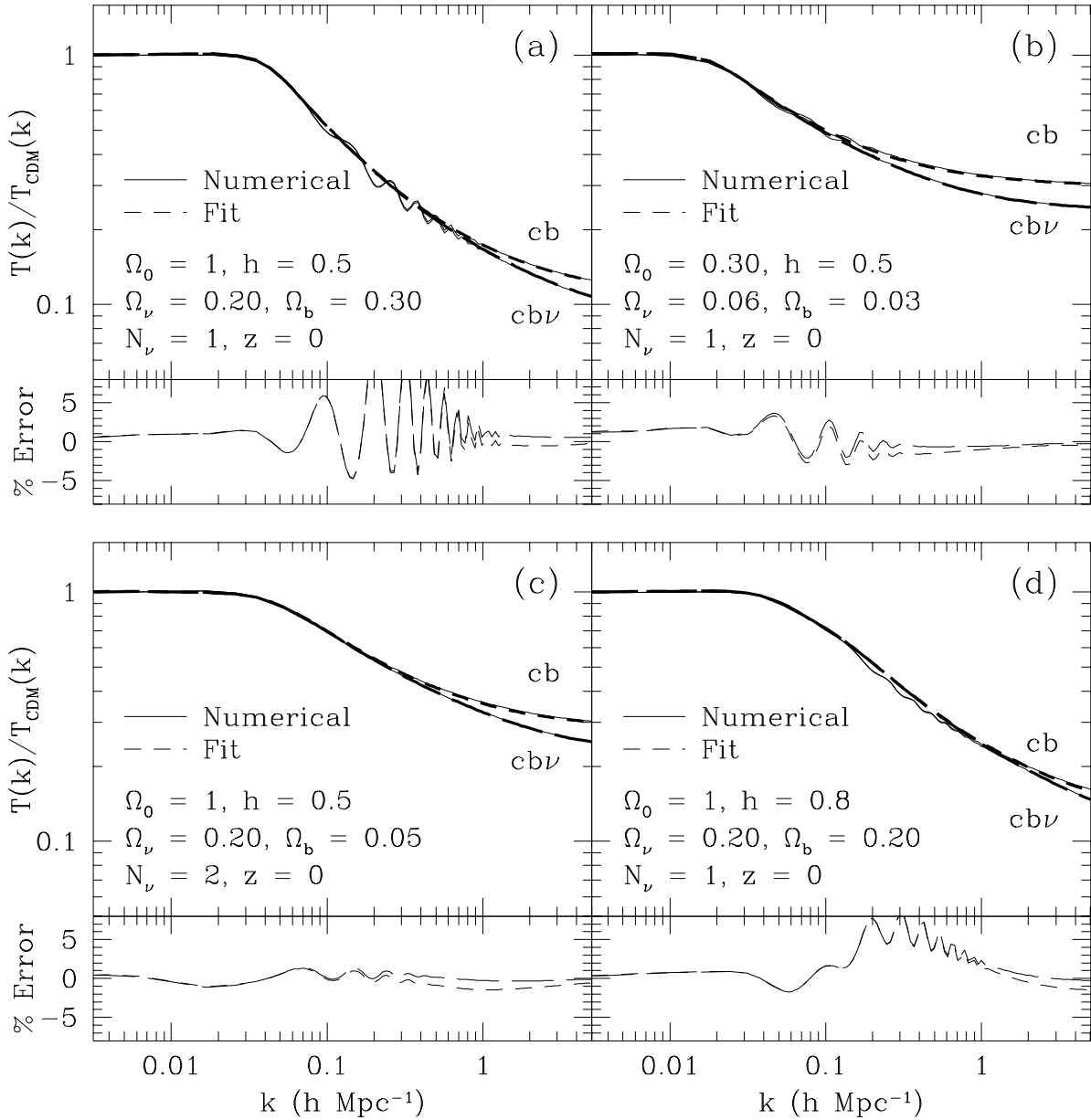


FIG. 2.—Same as Fig. 1, but for different choices of cosmology. (a) High-baryon model, with $\Omega_b = 0.3$, $\Omega_\nu = 0.2$, $\Omega_0 = 1$, and $h = 0.5$. (b) Low-density, flat model with $\Omega_0 = 0.3$, $\Omega_\Lambda = 0.7$, $\Omega_\nu = 0.06$, $\Omega_b = 0.03$, and $h = 0.5$. (c) Model with two degenerate neutrino species ($N_\nu = 2$), $\Omega_b = 0.05$, $\Omega_\nu = 0.2$, $\Omega_0 = 1$, and $h = 0.5$. (d) Model with high $\Omega_0 h^2$, beyond our range of (0.06, 0.40). $\Omega_b = 0.2$, $\Omega_\nu = 0.2$, $\Omega_0 = 1$, and $h = 0.8$.

with $f_0(z)$ as the value of f in the absence of free streaming:

$$f_0(z) \equiv -\frac{d \log D_1}{d \log(1+z)} \approx \Omega(z)^{0.6} + \frac{1}{70} \Omega_\Lambda(z) \left[1 + \frac{\Omega(z)}{2} \right], \quad (28)$$

where the approximation (Lahav et al. 1991) uses $\Omega(z)$ and $\Omega_\Lambda(z)$ from equation (10).

The power spectrum for the velocity field for the CDM and baryons is then

$$P_{cb}^{(v)}(k, z) = \left[\frac{f_{cb}(k, z) H_0 g(z)}{(1+z)k} \right]^2 P_{cb}(k, z), \quad (29)$$

where $g(z)$ was defined in equation (9). A similar relation follows for the velocity field of the density-weighted matter.

4.2. COBE Normalization

To normalize the power spectrum to the COBE Differential Microwave Radiometer measurement, one may use the fitting formulae of Bunn & White (1997) to fix δ_H . For cases with no CMB anisotropies from gravitational waves, one has

$$\delta_H = 1.94 \times 10^{-5} \Omega_0^{-0.785 - 0.05 \ln \Omega_0} e^{-0.95\bar{n} - 0.169\bar{n}^2}, \quad \Lambda = 1 - \Omega_0, \quad (30)$$

$$\delta_H = 1.95 \times 10^{-5} \Omega_0^{-0.35 - 0.19 \ln \Omega_0 - 0.17\bar{n}} e^{-\bar{n} - 0.14\bar{n}^2}, \quad \Lambda = 0, \quad (31)$$

valid for $0.7 \leq n \leq 1.2$. For flat cosmologies with the gravitational wave contributions of power-law inflation (which

requires $n < 1$), δ_H is

$$\delta_H = 1.94 \times 10^{-5} \Omega_0^{-0.785 - 0.05 \ln \Omega_0} e^{\tilde{n} + 1.97\tilde{n}^2},$$

$$\Lambda = 1 - \Omega_0. \quad (32)$$

For open cosmologies with the minimal gravitational wave contribution from power-law inflation (again, $n < 1$), one has (Hu & White 1997)

$$\delta_H = 1.95 \times 10^{-5} \Omega_0^{-0.35 - 0.19 \ln \Omega_0 - 0.15\tilde{n}} e^{1.02\tilde{n} + 1.70\tilde{n}^2},$$

$$\Lambda = 0. \quad (33)$$

In all cases, $\tilde{n} = n - 1$ and the fits extend from $0.2 \leq \Omega_0 \leq 1$. The 1σ statistical uncertainty in the *COBE* normalization is 7%, primarily due to cosmic variance.

4.3. Mass Fluctuation Measures

The rms amplitude of mass fluctuations inside a particular spherically symmetric window is

$$\sigma_R = \left[\int_0^\infty \frac{dk}{k} \frac{k^3}{2\pi^2} P(k) |\tilde{W}_R(k)|^2 \right]^{1/2}, \quad (34)$$

where $P(k)$ is the power spectrum and $\tilde{W}_R(k)$ is the Fourier transform of the real-space window function $W_R(r)$. Either P_{cb} or P_{cbv} may be used depending on the application. The two most popular choices for window functions are the real-space spherical top hat of radius R ,

$$W_R(r) \propto \begin{cases} 1 & \text{if } r \leq R, \\ 0 & \text{otherwise,} \end{cases} \quad (35)$$

$$\tilde{W}_R(k) = \frac{3}{(kR)^3} (\sin kR - kR \cos kR), \quad (36)$$

$$M_R = \frac{4\pi}{3} \rho_c \Omega_0 R^3, \quad (37)$$

and the Gaussian window of scale length R ,

$$W_R(r) \propto \exp\left(-\frac{r^2}{2R^2}\right), \quad (38)$$

$$\tilde{W}_R(k) = \exp\left[-\frac{(kR)^2}{2}\right], \quad (39)$$

$$M_R = (2\pi)^{3/2} \rho_c \Omega_0 R^3. \quad (40)$$

Here, M_R is the mass included in the window.

5. OBSERVATIONAL CONSTRAINTS

The fitting formula presented in § 3 allows one to manipulate statistics of the power spectrum as functions of cosmological parameters much more easily than a suite of Boltzmann integrations would allow. As examples of its use, we consider predictions for the power spectrum of large-scale structure, the abundance of clusters of galaxies, damped Ly α systems, and the Ly α forest. The theoretical power spectrum is related to these observations via the rms amplitude of mass fluctuations (§ 4.3) on various scales.

We consider two-dimensional cross sections in parameter space by varying the baryon and massive neutrino fractions in four fiducial models: the standard case of $\Omega_0 = 1$, $h = 0.5$, $n = 1$, and $N_\nu = 1$; a tilted variant with $n = 0.95$, and a tensor contribution to the CMB anisotropy; a variant with a second neutrino species ($N_\nu = 2$); and a low-density

flat universe with $\Omega_0 = 0.35$, $h = 0.7$, $n = 1$, and $N_\nu = 1$. We choose these models in order to explore the various ways of addressing what has been identified as the key problem of standard CDM (i.e., $\Omega_0 = 1$, $h = 0.5$, $n = 1$, and trace or zero baryon and neutrino content), namely, the overproduction of power on galaxy and cluster scales relative to larger scales (see, e.g., Efstathiou, Bond, & White 1992; Ostriker 1993; Dodelson, Gates, & Turner 1996b). As explained in § 3, adding massive neutrinos (Schaefer & Shafi 1992; Davis, Summers, & Schlegel 1992; Taylor & Rowan-Robinson 1992; Holtzman & Primack 1992) or baryons (White et al. 1996) reduces small-scale power. This alone may be sufficient to satisfy constraints. However, other simple extensions act to suppress power and may produce a better fit to the data. Adding a red tilt ($n < 1$) to the initial power spectrum (see, e.g., Cen et al. 1992) or lowering the density parameter Ω_0 (see, e.g., Efstathiou et al. 1992; Ostriker & Steinhardt 1995) are common approaches. We also consider the addition of a second species of massive neutrinos (Primack et al. 1995); this helps because it further reduces power on cluster scales while leaving the small-scale power essentially unchanged.

5.1. Power Spectrum Shape

We begin at large scales and consider the shape of the linear power spectrum as reconstructed from galaxy surveys. Peacock & Dodds (1994) considered a collection of data sets vis-à-vis zero baryon power spectrum models; they found that scale-invariant models with $\Gamma \equiv \Omega_0 h = 0.255 \pm 0.017$ provided the best fit. However, adding baryons and/or neutrinos alters the shape and hence the best fit. We do not perform this detailed reanalysis here; rather, we use the ratio of large- to small-scale power as a proxy for the shape (see, e.g., White et al. 1996). In particular, we construct the ratio of the amplitude of density-weighted fluctuations (P_{cbv}) within a $50 h^{-1}$ Mpc top hat to those within a $8 h^{-1}$ Mpc top hat; i.e., σ_{50}/σ_8 . The range $\Gamma = 0.25 \pm 0.05$, which we conservatively adopt, converts to $\sigma_{50}/\sigma_8 = 0.151 \pm 0.016$. Note that high values of Γ produce lower values of σ_{50}/σ_8 .

We display this ratio in Figures 3a–3d (*left panel*) as a function of baryon fraction and neutrino fraction. It is important to note that baryons play as important a role as neutrinos in suppressing power on cluster scales relative to larger scales (White et al. 1996). For example, even the cosmic concordance model (Ostriker & Steinhardt 1995) of $\Omega_0 = 0.35$ with $h = 0.7$, which seems to have an appropriate Γ , stretches the constraint when pushed to the 10%–15% baryon fraction suggested by cluster mass determinations (see, e.g., White et al. 1993b; David, Jones, & Forman 1995; White & Fabian 1995; Evrard 1997).

5.2. Cluster Abundance

The present-day abundance of rich clusters of galaxies is a sensitive probe of mass fluctuations on the $8 h^{-1}$ Mpc scale (Evrard 1989; White, Efstathiou, & Frenk 1993a; Eke, Cole, & Frenk 1996; Viana & Liddle 1996; Bond & Myers 1996; Pen 1998). We adopt the determination of Pen (1998),

$$\sigma_8 \approx 0.5 \Omega_0^{-0.65}, \quad (41)$$

and take a conservative range of 30% errors (i.e., 0.5 ± 0.15).

The time evolution of the abundance of clusters provides a way to isolate σ_8 from its Ω_0 dependence (Carlberg et al.

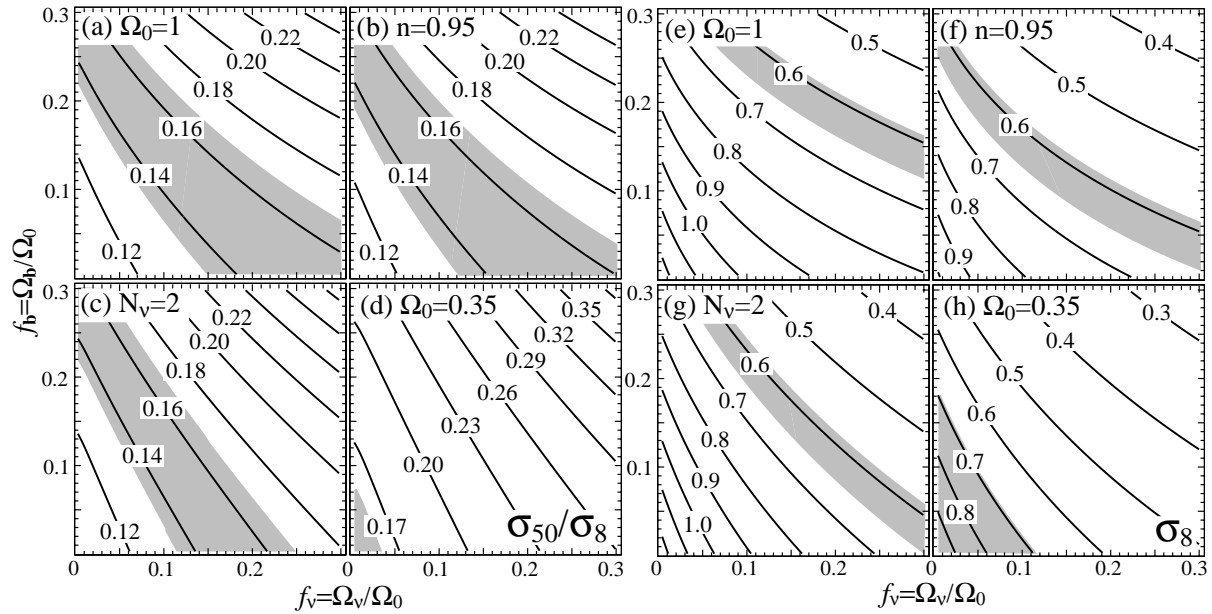


FIG. 3.—(a–d) Ratio of fluctuations within $50 h^{-1}$ Mpc spheres to that within $8 h^{-1}$ Mpc spheres as a function of neutrino and baryon fractions for various cosmologies. The shaded region shows the preferred range of $\sigma_{50}/\sigma_8 = 0.151 \pm 0.016$. (a) $\Omega_0 = 1$, $h = 0.5$, $n = 1$, and $N_\nu = 1$. (b) As in (a), but with $n = 0.95$ and tensors as per power-law inflation. (c) As in (a), but with two degenerate neutrino species ($N_\nu = 2$). (d) $\Omega_0 = 0.35$, $\Omega_\Lambda = 0.65$, $h = 0.7$, $n = 1$, and $N_\nu = 1$. All are *COBE* normalized. (e–h) Amplitude of fluctuations within $8 h^{-1}$ Mpc spheres for the cosmologies given in (a–d), respectively. The shaded region is the preferred range of $\sigma_8 = (0.5 \pm 0.15)\Omega_0^{-0.65}$ (Pen 1998) and $\sigma_8 > 0.59$ (Fan et al. 1997).

1997; Fan, Bahcall, & Cen 1997). By comparing the abundance of high-redshift clusters relative to the present-day abundance, Fan et al. (1997) found $\sigma_8 = 0.83 \pm 0.15$ (1 σ). To be conservative, we employ a 2σ lower limit (from the relevant quantity σ_8^2) of $\sigma_8 > 0.59$.

Figures 3e–3h (right panel) shows the cluster abundance constraints for the same four models as Figures 3a–3d. As is well known, high- Ω_0 cosmologies with small tilt and trace baryon and neutrino content overproduce present-day clusters. Adding a substantial fraction of baryons or neutrinos makes the models marginally consistent with both the present-day and high-redshift cluster abundances.

5.3. Damped Ly α Systems

Cosmologies with moderate neutrino fractions have a strong suppression of power on small scales. This implies that they form protogalactic systems later than pure CDM models. Indeed, these models may have trouble forming high-redshift objects such as quasars (see, e.g., Ma & Bertschinger 1994; Liddle et al. 1996), UV-dropout galaxies (Mo & Fukugita 1996), and damped Ly α systems (Mo & Miralda-Escudé 1994; Ma & Bertschinger 1994; Kauffmann & Charlot 1994; Klypin et al. 1995). We focus on the last of these.

Observations of damped Ly α absorption systems in QSO spectra may be interpreted as a measurement of the mean density of neutral hydrogen, Ω_{gas} , in units of the critical density. Recent measurements at $z = 4$ (Storrie-Lombardi, Irwin, & McMahon 1996) find this to be

$$\Omega_{\text{gas}}(z \approx 4) = (9.3 \pm 3.8) \times 10^{-4} h^{-1} [(1+z)^{3/2} g(z)] \Big|_{z=4}. \quad (42)$$

Assuming Poisson statistics, we adopt a 95% lower limit of 43% of the central value.

One can estimate an upper limit to the value of Ω_{gas} in a particular cosmology by assuming that all gas in protogalactic halos is neutral and by using the Press-Schechter formalism (Press & Schechter 1974) to estimate the number of such halos (Mo & Miralda-Escudé 1994; Kauffmann & Charlot 1994; Ma & Bertschinger 1994; Klypin et al. 1995; Liddle et al. 1996). These works differ in their Press-Schechter implementation; here we adopt the conservative assumptions of Klypin et al. (1995). We define σ_{DLA} to be the amplitude of fluctuations (using P_{cbv}) inside a Gaussian window of a scale corresponding to a circular velocity v_c of $50 \text{ km s}^{-1} \text{ Mpc}^{-1}$. The relation between mass and velocity is (Narayan & White 1987)

$$M = \frac{v_c^3}{\sqrt{89GH_0} g(z)}, \quad (43)$$

where $g(z)$ is defined in equation (9). Then the density of neutral gas arising from all halos with velocities greater than $50 \text{ km s}^{-1} \text{ Mpc}^{-1}$ is

$$\Omega_{\text{gas}} = f_{\text{HI}} \Omega_b \text{erfc} \left(\frac{\delta_c}{\sqrt{2}\sigma_{\text{DLA}}} \right), \quad f_{\text{HI}} \leq 1 \quad (44)$$

where f_{HI} is the fraction of neutral gas, $\text{erfc}(x)$ is the complementary error function, and we take a density threshold of $\delta_c = 1.33$.

In Figures 4a–4d (left panel), we plot σ_{DLA} as a function of cosmological parameters. We superpose the constraint implied by comparing equation (42) to equation (44) with $f_{\text{HI}} = 1$. As found by previous studies, MDM models with $f_\nu \gtrsim 0.3$ underproduce high-redshift halos; the constraints are tighter for higher f_b , red-tilted, and degenerate-neutrino models. The limits in Figure 4 are actually extremely conservative; hydrodynamical studies (Ma et al. 1997; Gardner et al. 1997a, 1997b) infer $f_{\text{HI}} \lesssim 0.1$ in tested cases. Correspondingly, we plot the limits of $f_{\text{HI}} = 0.1$ in dashed lines to

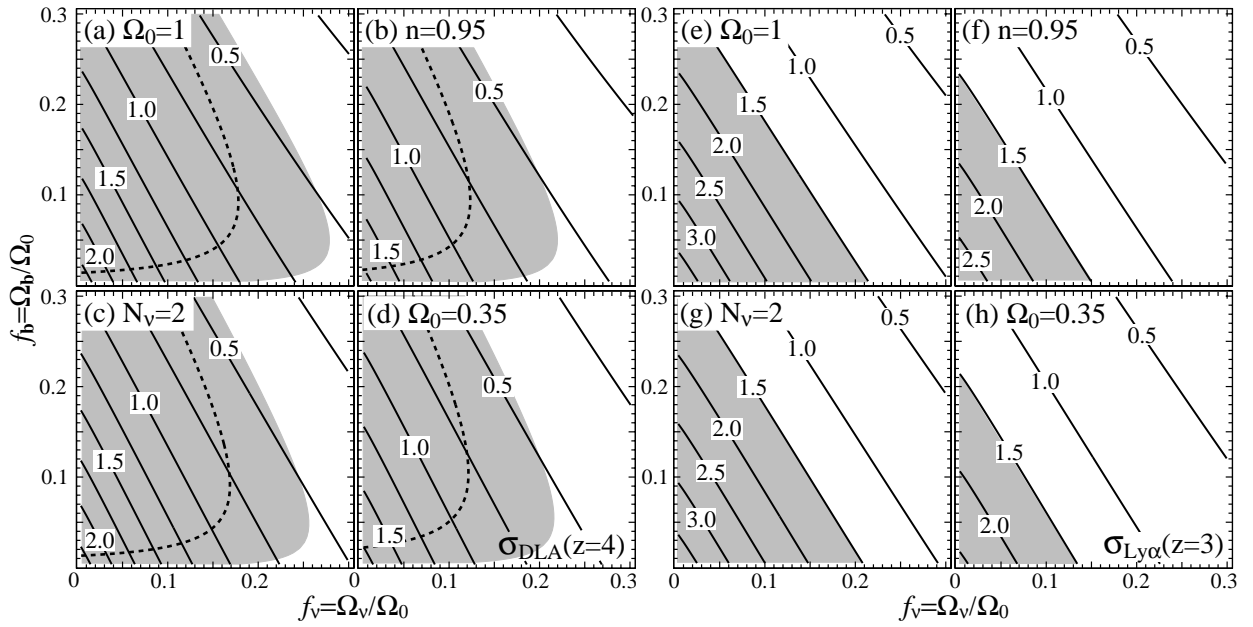


FIG. 4.—(a–d) Amplitude of fluctuations at $\sigma_{\text{DLA}}(z=4)$ within a Gaussian window of mass corresponding to halos of $50 \text{ km s}^{-1} \text{ Mpc}^{-1}$ circular velocity. Cosmologies are as per Fig. 3. The shaded region indicates cosmologies where the neutral gas in halos of $v_c > 50 \text{ km s}^{-1} \text{ Mpc}^{-1}$ (using the prescription of Klypin et al. 1995 and $f_{\text{HI}} = 1$) exceeds that observed in damped Ly α systems. The region to the left of the dashed line is the allowed region for $f_{\text{HI}} = 0.1$. (e–h) Amplitude of fluctuations at $\sigma_{\text{Ly}\alpha}(z=3)$ for a Gaussian window of radius $0.0416(\Omega_0 h^2)^{-1/2} \text{ Mpc}$, suggested by Gnedin (1997) as an indicator of the slope of the column-density distribution of the Ly α forest. The region $\sigma_{\text{Ly}\alpha} > 1.5$ is shaded. Cosmologies are as in Fig. 3.

show how this uncertainty affects the cosmological constraints. Since it is difficult to scale these numerical corrections as functions of cosmological parameters, especially if varying Ω_b (Gardner et al. 1997b), the $f_{\text{HI}} = 0.1$ line should not be taken as a firm constraint.

5.4. Ly α Forest

If the low column density absorption features in QSO spectra arise from mild density and velocity perturbations in the intergalactic medium (IGM; Cen et al. 1994; Pettjean, Mücke, & Kates 1995; Zhang, Anninos, & Norman 1995; Zhang et al. 1998; Miralda-Escudé et al. 1996; Hernquist et al. 1996), then the correlations and column-density distribution of the lines may yield robust information about the power spectrum on sub-Mpc scales. Croft et al. (1998) demonstrated that the power spectrum of simulations could be reconstructed from absorption spectra drawn from them. Gnedin (1998) showed that the power-law exponent of the column density distribution in various cosmological simulations is strongly correlated with the amplitude of linear fluctuations on the smallest collapsing scales. Comparing to the observed distribution suggests a lower bound on the amplitude of fluctuations on mass scales near $10^9 M_\odot$ at $z = 3$. In particular, the quantity $\sigma_{\text{Ly}\alpha}$, defined as the fluctuations inside a Gaussian window of radius $R = 0.0416(\Omega_0 h^2)^{-1/2} \text{ Mpc}$ using P_{cb} , is constrained to be greater than 1.5 at $z = 3$. The scale is chosen to approximate the Jeans length at $z = 3$ for common thermal histories (Gnedin 1998). This constraint is plotted in Figures 4e–4h (right panel).

5.5. Summary

Even in the standard *COBE*-normalized, $n = 1$, $\Omega_0 = 1$ model the inclusion of a moderate fraction of baryons or neutrinos can decrease σ_8 to an appropriate level. Models that accomplish this by the neutrino fraction alone produce

insufficient power to explain damped Ly α absorption systems. Models that accomplish this by the baryon fraction alone require baryon densities far in excess of big bang nucleosynthesis predictions. Although a compromise of $\Omega_b = 0.15$ and $\Omega_v = 0.25$ would work, Figure 3 shows that no model in this scenario fits the σ_{50}/σ_8 and σ_8 constraints.

However, the modest change of altering the tilt to 0.95 (with tensors) or adding a second degenerate neutrino species opens regions of parameter space that match both large-scale structure and constraints from damped Ly α systems. For example, models with $\Omega_b = 0.1$, $h = 0.5$, and either $\Omega_v = 0.15$ with $n = 0.95$ or $\Omega_v = 0.2$ with $N_v = 2$ produce $\sigma_8 \approx 0.64$ and match the high-redshift constraints with $f_{\text{HI}} \sim 0.2$. $f_{\text{HI}} \approx 0.1$ could be achieved by reducing the *COBE* normalization by 7% (a $1 - \sigma$ shift) and decreasing Ω_v so as to keep σ_8 constant. The higher value of Ω_b —as compared with the canonical value of 0.05 from Walker et al. (1991) but in agreement with Tytler, Fan, & Burles (1996)—is doubly useful in meeting the requirements: the suppression due to baryons occurs at larger scales than that from neutrinos and therefore alters σ_8 more effectively, while the additional baryons are available to produce high-redshift absorption. Moreover, this value of Ω_b better agrees with the baryon fraction in clusters (see, e.g., White et al. 1993b; David et al. 1995; White & Fabian 1995; Evrard 1997) and that inferred from the Ly α forest (see, e.g., Miralda-Escudé et al. 1996; Weinberg et al. 1997; Zhang et al. 1998).

The more common solution to the problems of $\Omega_0 = 1$ CDM is to reduce the value of Ω_0 to around 0.3. As shown in Figures 3 and 4, this satisfies the quoted constraints when used with small baryon and neutrino fractions. An important lesson of the figures, however, is that small admixtures of baryons or neutrinos can make significant changes. For example, the $\Omega_0 = 0.35$ flat model presented here tends to underproduce power even with only a 10% baryon fraction

($\Omega_b h^2 = 0.017$). The lack of small-scale power in such models places more stringent limits on Ω_v/Ω_0 than in high-density cosmologies; this implies a stronger limit for the neutrino mass $m_\nu \propto \Omega_v h^2$. Of course, a small blue tilt would help the situation.

It is very interesting to note that early results from modeling the Ly α forest (§ 5.4, Figs. 4e–4h) are more effective at excluding models than constraints from damped systems. The limits suggested by Gnedin (1998) would eliminate all of the $\Omega_0 = 1$ models studied in Figures 3 and 4. Perhaps models with blue tilts ($n > 1$) would succeed in producing sufficient amounts of small-scale power, although of course they would require more suppression of power at cluster scales relative to *COBE*. Constraints from the Ly α forest are still only preliminary, but they appear to be quite promising.

6. CONCLUSION

In this paper, we have considered adiabatic models composed of baryons, CDM, and massive neutrinos. We have presented a fitting formula for the linear transfer function of such models, including the possibility of $\Omega_0 \neq 1$ and multiple degenerate neutrino models. The parameter space covered by the formula is much larger than that previously available; we provide functions of space, time, and six cosmological parameters. The accuracy is $\lesssim 5\%$ in the central range of $0.06 \lesssim \Omega_0 h^2 \lesssim 0.40$, $\Omega_b/\Omega_0 \leq 0.3$, $\Omega_v/\Omega_0 \leq 0.3$, and $z < 30$ and improves to $\lesssim 3\%$ for models with baryon fractions below 10%.

An accurate, general fitting formula allows one to calculate statistics of the power spectrum as functions of cosmological parameters quite efficiently. As an example of this, we presented several different observational tests and displayed the constraints as functions of baryon fraction and neutrino fraction for various choices of the other cosmological parameters. Baryons and neutrinos are both effective at suppressing small-scale power relative to that on larger scales. We find that models with large baryon fractions are less “observationally challenged,” in that a given reduction

on cluster scales (i.e., σ_8) imposes less suppression on very small scales where power is needed to produce damped Ly α systems and other high-redshift objects. Hence if Ω_b is as large as 0.1, as suggested by Tytler et al. (1996) for $h = 0.5$, then constraints on MDM models are weakened. For example, with a tilt of $n = 0.95$, an MDM model with $\Omega_v = 0.15$ and $\Omega_b = 0.1$ fares significantly better than one with $\Omega_v = 0.2$ and $\Omega_b = 0.05$. Finally, we find that the constraint on the small-scale power as derived from the slope of the column-density distribution of the Ly α forest (Gnedin 1998) is an extremely powerful limit on MDM models. Further work is needed to test the robustness of this inference.

The observations discussed above place constraints upon the neutrino mass, although these limits vary with other presently unknown parameters, e.g., Ω_0 , h , Ω_b , and n . Future CMB observations should precisely determine these quantities (Jungman et al. 1996; Bond, Efstathiou, & Tegmark 1997; Zaldarriaga, Spergel, & Seljak 1997) but will have little leverage on Ω_v (Ma & Bertschinger 1995; Dodelson et al. 1996a). However, the combination of CMB data with large-scale structure observations will allow a robust determination of Ω_v . Further observations and modeling of damped Ly α systems and the Ly α forest will corroborate this but may not be clean enough to yield a precise measurement. If Ω_0 is found to be low, our sensitivity to the neutrino mass will be stronger because the suppression of small-scale power depends on Ω_v/Ω_0 ; this differs from the trend in the CMB, where lowering Ω_0 shifts the effects of neutrinos to smaller angular scales. This illustrates the power of combining cosmological data sets with regard to determining the properties of the dark matter.

We thank J. Phillips, D. Spergel, M. White, and M. Zaldarriaga for useful discussions. D. J. E. is a Frank and Peggy Taplin Member at the IAS and is additionally supported by NSF-9513835. W. H. is supported by the W. M. Keck Foundation and NSF-9513835. Numerical results were taken from the CMB fast package of Seljak & Zaldarriaga (1996).

REFERENCES

- Achilli, S., Occhionero, F., & Scaramella, R. 1985, *ApJ*, 299, 577
 Bardeen, J. M., Bond, J. R., Kaiser, N., & Szalay, A. S. 1986, *ApJ*, 304, 15
 Bildhauer, S., Buchert, T., & Kasai, M. 1992, *A&A*, 263, 23
 Bond, J. R., & Efstathiou, G. 1984, *ApJ*, 285, L45
 Bond, J. R., Efstathiou, G., & Silk, J. 1980, *Phys. Rev. Lett.*, 45, 1980
 Bond, J. R., Efstathiou, G., & Tegmark, M. 1997, *MNRAS*, 291, L33
 Bond, J. R., & Myers, S. T. 1996, *ApJS*, 103, 63
 Bond, J. R., & Szalay, A. 1983, *ApJ*, 276, 443
 Bunn, E. F., & White, M. 1997, *ApJ*, 480, 6
 Carlberg, R. G., Morris, S. L., Yee, H. K. C., & Ellingson, E. 1997, *ApJ*, 479, L19
 Carroll, S. M., Press, W. H., & Turner, E. L. 1992, *ARA&A*, 30, 499
 Cen, R., Gnedin, N. Y., Kofman, L. A., & Ostriker, J. P. 1992, *ApJ*, 399, L11
 Cen, R., Miralda-Escudé, J., Ostriker, J. P., & Rauch, M. 1994, *ApJ*, 437, L9
 Croft, R. A. C., Weinberg, D. H., Katz, N., & Hernquist, L. 1998, *ApJ*, 495, 44
 David, L. P., Jones, C., & Forman, W. 1995, *ApJ*, 445, 578
 Davis, M., Summers, F., & Schlegel, D. 1992, *Nature*, 359, 393
 Dodelson, S., Gates, E., & Stebbins, A. 1996a, *ApJ*, 467, 10
 Dodelson, S., Gates, E., & Turner, M. S. 1996b, *Science*, 274, 69
 Edwards, D., & Heath, D. 1976, *Ap&SS*, 41, 183
 Efstathiou, G., Bond, J. R., & White, S. D. M. 1992, *MNRAS*, 258, 1P
 Eisenstein, D. J., & Hu, W. 1998, *ApJ*, 496, 605 (EH98)
 Eke, V. R., Cole, S., & Frenk, C. S. 1996, *MNRAS*, 282, 263
 Evrard, A. E. 1989, *ApJ*, 341, L71
 ———. 1997, *MNRAS*, 292, 289
 Fang, L. Z., Li, S. X., & Xiang, S. P. 1984, *A&A*, 140, 77
 Fan, X., Bahcall, N., & Cen, R. 1997, *ApJ*, 490, L123
 Fixsen, D., et al. 1996, *ApJ*, 473, 576
 Gardner, J. P., Katz, N., Weinberg, D. H., & Hernquist, L. 1997a, *ApJ*, 484, 31
 ———. 1997b, *ApJ*, 486, 42
 Gnedin, N. Y. 1998, *MNRAS*, 299, 392
 Groth, E. J., & Peebles, P. J. E. 1975, *A&A*, 41, 143
 Heath, D. J. 1977, *MNRAS*, 179, 351
 Hernquist, L., Katz, N., Weinberg, D. H., & Miralda-Escudé, J. 1996, *ApJ*, 457, L51
 Holtzman, J. A. 1989, *ApJS*, 71, 1
 Holtzman, J. A., & Primack, J. R. 1993, *ApJ*, 405, 428
 Hu, W., & Eisenstein, D. J. 1998, *ApJ*, 498, 497 (HE98)
 Hu, W., & Sugiyama, N. 1996, *ApJ*, 471, 542
 Hu, W., & White, M. 1997, *ApJ*, 486, L1
 Jungman, G., Kamionkowski, M., Kosowsky, A., & Spergel, D. N. 1996, *Phys. Rev.*, 54, 1332
 Kauffmann, G., & Charlot, S. 1994, *ApJ*, 430, L97
 Klypin, A., Borgani, S., Holtzman, J. A., & Primack, J. R. 1995, *ApJ*, 441, 1
 Klypin, A., Holtzman, J., Primack, J., & Regös, E. 1993, *ApJ*, 416, 1
 Kolb, E. W., & Turner, M. S. 1990, *The Early Universe* (Redwood City: Addison-Wesley)
 Lahav, O., Rees, M. J., Lilje, P. B., & Primack, J. R. 1991, *MNRAS*, 251, 128
 Liddle, A., et al. 1996, *MNRAS*, 281, 531
 Ma, C.-P. 1996, *ApJ*, 471, 13
 Ma, C.-P., & Bertschinger, E. 1994, *ApJ*, 434, L5
 ———. 1995, *ApJ*, 455, 7
 Ma, C.-P., Bertschinger, E., Hernquist, L., Weinberg, D. H., & Katz, N. 1997, *ApJ*, 484, L1
 Miralda-Escudé, J., Cen, R., Ostriker, J. P., & Rauch, M. 1996, *ApJ*, 471, 582
 Mo, H. J., & Fukugita, M. 1996, *ApJ*, 467, L9

- Mo, H. J., & Miralda-Escudé, J. 1994, *ApJ*, 430, L25
Narayan, R., & White, S. D. M. 1987, *MNRAS*, 231, 97P
Ostriker, J. P. 1993, *ARA&A*, 31, 689
Ostriker, J. P., & Steinhardt, P. J. 1995, *Nature*, 377, 600
Peacock, J. A., & Dodds, S. J. 1994, *MNRAS*, 267, 1020
Peebles, P. J. E. 1980, *Large-Scale Structure of the Universe* (Princeton: Princeton Univ. Press)
———. 1993, *Principles of Physical Cosmology* (Princeton: Princeton Univ. Press), § 25
Pen, U.-L. 1998, *ApJ*, 498, 1
Petitjean, P., Mücke, J. P., & Kates, R. 1995, *A&A*, 295, L9
Pogosyan, D. Yu., & Starobinsky, A. A. 1995, *MNRAS*, 447, 465
Press, W. H., & Schechter, P. L. 1974, *ApJ*, 197, 425
Primack, J. R., Holtzman, J., Klypin, A., & Caldwell, D. O. 1995, *Phys. Rev. Lett.*, 74, 2160
Schaefer, R. K., & Shafi, Q. 1992, *Nature*, 358, 199
Seljak, U., & Zaldarriaga, M. 1996, *ApJ*, 469, 437
Storrie-Lombardi, L. J., Irwin, M. J., & McMahon, R. G. 1996, *MNRAS*, 283, L79
Taylor, A. N., & Rowan-Robinson, M. 1992, *Nature*, 359, 396
Tytler, D., Fan, X. M., & Burles, S. 1996, *Nature*, 381, 207
Valdarnini, R., & Bonometto, S. A. 1985, *A&A*, 146, 235
Viana, P. T. P., & Liddle, A. R. 1996, *MNRAS*, 281, 323
Walker, T. P., Steigman, G., Kang, H., Schramm, D. M., & Olive, K. A. 1991, *ApJ*, 376, 51
Weinberg, D. H., Miralda-Escudé, J., Hernquist, L., & Katz, N. 1997, *ApJ*, 490, 564
Weinberg, S. 1972, *Gravitation and Cosmology* (New York: Wiley)
White, D. A., & Fabian, A. C. 1995, *MNRAS*, 273, 72
White, M., Viana, P., Liddle, A., & Lyth, D. 1996, *MNRAS*, 283, 107
White, S. D. M., Efstathiou, G., & Frenk, C. S. 1993a, *MNRAS*, 262, 1023
White, S. D. M., Navarro, J. F., Evrard, A. E., & Frenk, C. S. 1993b, *Nature*, 366, 429
Yamamoto, K., Sugiyama, N., & Sato, H. 1998, *ApJ*, 501, 442
Zaldarriaga, M., Spergel, D. N., & Seljak, U. 1997, *ApJ*, 488, 1
Zhang, Y., Anninos, P., & Norman, M. L. 1995, *ApJ*, 453, L57
Zhang, Y., Meiksin, A., Anninos, P., & Norman, M. L. 1998, *ApJ*, 495, 63